社団法人　電子情報通信学会
THE INSTITUTE OF ELECTRONICS,
INFORMATION AND COMMUNICATION ENGINEERS

信学技報
TECHNICAL REPORT OF IEICE.

CIP-FDTDハイブリッド法の分散性による数値誤差についての検討

チャカロタイ　ジェドヴィスノプ†　　陳　強†　　澤谷　邦男†

† 東北大学大学院 工学研究科 電気通信工学専攻　〒 980–8579 仙台市青葉区荒巻字青葉 05
E-mail: †jerd@ecei.tohoku.ac.jp

あらまし　近年，電磁界解析手法として CIP 法が新しく提案され，従来の FDTD 法と比較して数値分散特性が優れているという点が注目を浴びている．しかし，解析領域内にアンテナを含む計算は CIP 法におけるセル内の電磁界が全て同じ位置にあるため，解が不安定となりやすい．そこで本論文では，アンテナを含んだ長距離伝搬空間の解析手法として FDTD 法と CIP 法を組み合わせた CIP-FDTD ハイブリッド法を新たに提案する．CIP 及び FDTD 領域との間に平均法を用いた境界条件を設け，境界からの反射量を求めた．また CIP-FDTD ハイブリッド法の数値分散特性を評価し，FDTD 法及び CIP 法との比較検討を行った．

キーワード　電磁界解析，長距離伝搬，ハイブリッド法，CIP 法，FDTD 法，数値分散，位相誤差

Study on Numerical Dispersion Error of Hybrid CIP-FDTD Method

Jerdvisanop CHAKAROTHAI†, Qiang CHEN†, and Kunio SAWAYA†

† Electrical and Communication Engineering, Graduate School of Engineering, Tohoku University
05 Aoba, Aramaki-Aza, Aoba-ku, Sendai-shi, 980–8579 Japan
E-mail: †jerd@ecei.tohoku.ac.jp

Abstract　Although the contrained interpolation profile (CIP) method has a smaller numerical dispersion when compared with the standard Yee's finite difference time domain (FDTD) algorithm, the electric and magnetic field arrangements of CIP method make it difficult to model antennas into the analysis space. A hybridization of CIP method and FDTD method is proposed to solve the problems of large- or long-distance propagation space including antennas in this paper. The boundary conditions between CIP and FDTD method are also considered and validated. The results show that the numerical dispersion of the hybrid CIP-FDTD method is almost same as that of the CIP method, which is superior to that of the FDTD method.

Key words　Electromagnetic Wave Propagation, Phase Error, CIP, FDTD, Numerical Analysis, Hybrid Method

1. Introduction

The Finite-Difference Time-Domain (FDTD) method has been widely used in the computational electromagnetics. However, Yee's FDTD method suffers from numerical dispersion. Since the velocity is a function of the direction of travel, the discretized medium is anisotropic. This anisotropy gives rise to a direction-dependent phase error [2]. These errors are accumulated as the numerical wave propagates, limiting the accuracy of FDTD for solving some problems, such as a long-distance propagation problem.

To reduce the error accumulation and increase the accuracy of time-domain solutions, many researchers have tried to improve FDTD algorithms that have smaller dispersion errors. One of this solutions is the larger computational stencil or higher-order finite differences method such as Ty(2,4) or Ty(2,6) scheme [3]〜[5]. However, the complexity of computation is increased and difficult treatments to the absorbing boundary condition are required.

The characteristic-based Contrained Interpolation Profile (CIP) method [6]- [8] proposed by Yabe and co-workers is applied to the computational electromagnetics because CIP method can accurately solve the hyperbolic equations with a small dispersion and stable scheme with third-order accuracy in space [9]. So many researchers have tried to solve the electromagnetic problems with CIP method [11]- [14]. However the arrangement of electric and magnetic fields which exist at the same location in CIP method makes it difficult to model an antenna into CIP region.

A hybridization of the CIP and FDTD methods with

a boundary condition between two regions in the two-dimensional space is proposed in this study. In the total analysis region, antennas are modelled in the FDTD region and empty space for wave propagation is implemented by CIP scheme. A suitable boundary condition between both regions is also developed. The reflection coefficient from the proposed boundary is numerically computed to verify the hybrid method. The phase error of the hybrid CIP-FDTD method is evaluated and compared to that of FDTD and CIP method.

2. Formulation of Maxwell equations including dielectric media for CIP method

In this section, the CIP algorithm for Maxwell equations in one dimension is explained [15]. One-dimensional Maxwell equations are described as

$$\frac{\partial E_y}{\partial t} + \frac{1}{\varepsilon}\frac{\partial H_z}{\partial x} = -\frac{\sigma}{\varepsilon}E_y \tag{1}$$

$$\frac{\partial H_z}{\partial t} + \frac{1}{\mu}\frac{\partial E_y}{\partial x} = 0 \tag{2}$$

where ε, μ and σ are the permittivity, permeability and the conductivity of the medium, respectively. To apply CIP algorithm, Eqs.(1) and (2) are modified by determining eigenvalues and eigenfunctions:

$$\frac{\partial F^{\pm}}{\partial t} \pm \lambda^{\pm}\frac{\partial F^{\pm}}{\partial x} = -\frac{\sigma}{\varepsilon}E_y \tag{3}$$

where, $F^{\pm} = E_y \pm \sqrt{\mu/\varepsilon}H_z$ is the invariant quantity of characteristics, $\lambda^{\pm} = 1/\sqrt{\varepsilon^{\pm}\mu^{\pm}}$ is the eigenvalue which represents the speed of light in each medium. However, Eq.(3) is not an absolute advection equation because there is a term of E_y left in the right side of the equation. Eq.(3) can be transformed using time splitting method as follows:

$$\frac{\partial F^{\pm}}{\partial t} \pm \lambda\frac{\partial F^{\pm}}{\partial x} = 0 \tag{4}$$

$$\frac{\partial F^{\pm}}{\partial t} = -\frac{\sigma}{\varepsilon}E_y \tag{5}$$

Now Eq.(4) can be calculated by CIP method because the equation is a complete advection equation and Eq.(5) is applied to the finite difference schemes.

When there are dielectrics in analysis space, there is a discontinuity between two different materials as shown in Fig.1 and the differences of the speed of light between two materials have to be taken into account in the calculation. The signs (+) and (-) denote the left and right characteristics of the intrinsic impedance and the speed of light of each material. The quantities of characteristics for each side can be represented as follows:

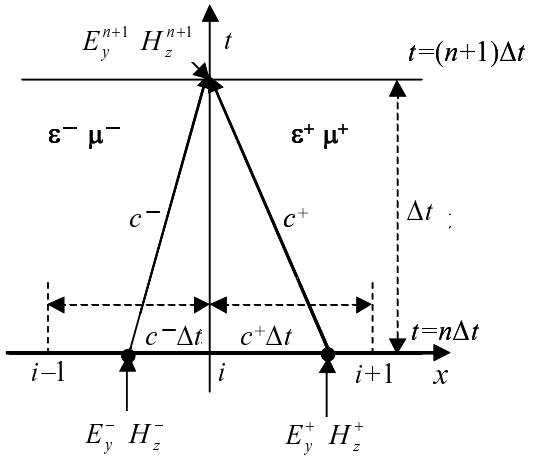

Fig. 1 Treatment of boundary between two different media

$$F^{n+} = E_y^{n+} + \sqrt{\frac{\mu^+}{\varepsilon^+}}H_z^{n+} \tag{6}$$

$$F^{n-} = E_y^{n-} - \sqrt{\frac{\mu^-}{\varepsilon^-}}H_z^{n-} \tag{7}$$

$$G^{n+} = \frac{\partial E_y^{n+}}{\partial x} + \sqrt{\frac{\mu^+}{\varepsilon^+}}\frac{\partial H_z^{n+}}{\partial x} \tag{8}$$

$$G^{n-} = \frac{\partial E_y^{n-}}{\partial x} - \sqrt{\frac{\mu^-}{\varepsilon^-}}\frac{\partial H_z^{n-}}{\partial x} \tag{9}$$

$F^{n\pm}$ and $G^{n\pm}$ are the quantities of characteristics in left and right media, respectively. These quantities are called Riemann's invariable quantities which do not change during the time development. Thus, the fields at the next step can be calculated by equating two invariant quantities.

$$E_y^{n\pm} \pm \sqrt{\frac{\mu^{\pm}}{\varepsilon^{\pm}}}H_z^{n\pm} = E_y^{\mathrm{cip}} \pm \sqrt{\frac{\mu^{\pm}}{\varepsilon^{\pm}}}H_z^{\mathrm{cip}} \tag{10}$$

So that $E_y^{n\pm}$ and $H_z^{n\pm}$ can be eventually calculated by following equations:

$$E_y^{\mathrm{cip}} = \frac{1}{\Omega_E}\left(\sqrt{\frac{\varepsilon^+}{\mu^+}}E_y^{n+} + \sqrt{\frac{\varepsilon^-}{\mu^-}}E_y^{n-} + H_z^{n+} - H_z^{n-}\right)$$

$$H_y^{\mathrm{cip}} = \frac{1}{\Omega_H}\left(E_y^{n+} - E_y^{n-} + \sqrt{\frac{\mu^+}{\varepsilon^+}}H_z^{n+} + \sqrt{\frac{\mu^-}{\varepsilon^-}}H_z^{n-}\right)$$

where,

$$\Omega_E = \frac{1}{\sqrt{\frac{\varepsilon^+}{\mu^+}} + \sqrt{\frac{\varepsilon^-}{\mu^-}}} \quad , \quad \Omega_H = \frac{1}{\sqrt{\frac{\mu^+}{\varepsilon^+}} + \sqrt{\frac{\mu^-}{\varepsilon^-}}}. \tag{11}$$

To calculate the nonadvection term represented by Eq.(5), the forward difference method is applied as follows:

$$E_y^{n+1} = \left(1 - \frac{\sigma}{\varepsilon}\Delta t\right)E_y^{\mathrm{cip}} \tag{12}$$

3. Boundary Condition between CIP and FDTD region

In the present analysis, FDTD method is used to the current sources and the CIP method is applied in the rest of

analysis region which do not include the source. Because the FDTD method uses the leapfrog arrangement of the field points of the electric and magnetic fields in the calculation but the field points in the CIP region are located at the same position in the cells, boundary condition at the interface between both two regions is required. The arrangement of electric and magnetic fields at the boundary condition is shown in Fig. 2. The field transition between FDTD and CIP methods is occured at the position i. The field components nearby the boundary interface is defined in the way shown in Fig. 3. First, the electric field component E_z of FDTD and CIP method are both located at the center of cells, so that the substutition can be done directly by $E_z^n|_{i,j}^{CIP} = E_z^n|_{i,j}^{FDTD}$. In order to obtain the magnetic field $H_x|^{CIP}$ and $H_y|^{CIP}$ at the position (i, j) in the hybrid region, average of the magnetic field components $H_x|^{CIP}$ and $H_y|^{CIP}$ are evaluated as follows:

$$H_x^n|_{i,j}^{CIP} = \frac{1}{2}\left(H_x^n|_{i,j-1/2}^{FDTD} + H_x^n|_{i,j+1/2}^{FDTD}\right), \quad (13)$$

$$H_y^n|_{i,j}^{CIP} = \frac{1}{2}\left(H_y^n|_{i-1/2,j}^{FDTD} + H_y^n|_{i-1/2,j}^{FDTD}\right), \quad (14)$$

The averaging method is also applied to the magnetic field components $H_x^{n-1/2}$, $H_x^{n+1/2}$, $H_y^{n-1/2}$ and $H_y^{n+1/2}$ because these components in the FDTD region do not exist at the time step n. After all of electric and magnetic field components at the boundary are retrieved from the FDTD region, they are used in the CIP region. It should be noted that the hybrid region is not included in the field calculation in this process, but its field values are applied for the computation of all field components at the position $(i + 1, j)$ in the CIP region. Then, the electric field component $E_z|_{i+1,j}^{CIP}$ is utilized to calculate the magnetic field $H_y|_{i+1/2,j}^{FDTD}$ by the ordinary Yee's algorithm according to the following update procedures:

$$H_y^{n+1/2}\Big|_{i+1/2,j}^{FDTD} = H_y^{n-1/2}\Big|_{i+1/2,j}^{FDTD} + \frac{\Delta t}{\mu \Delta x}\left(E_z^n|_{i+1,j}^{CIP} - E_z^n|_{i,j}^{FDTD}\right). \quad (15)$$

The electric and magnetic field components in both analysis regions are all computed by this process. It is required to save the magnetic field values of the last computation because the temporal averaging has to be done before the CIP calculation starts in the next step. Finally, the cyclic computation are done until the required time step N. Flowchart of the hybrid CIP-FDTD method is summarized in Fig. 4.

4. Numerical simulation and discussion

In this paper, the validation of the hybrid CIP-FDTD method with the proposed boundary condition is demonstrated and the investigation of its dispersion errors or phase error accumulation is also investigated and discussed by turns in the following subsections.

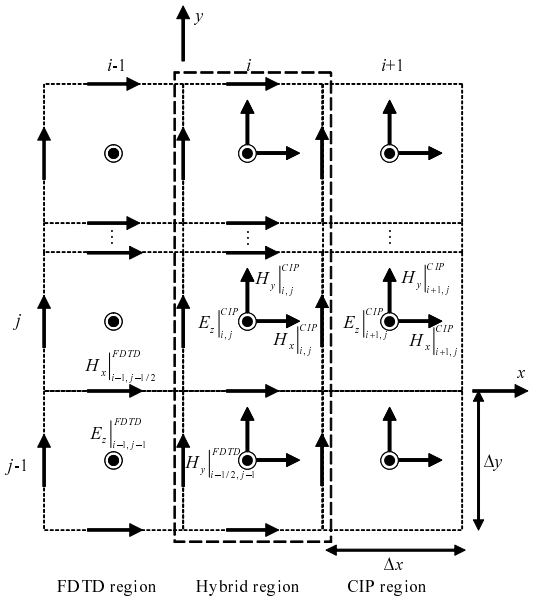

Fig. 2 The arrangement of electric and magnetic field components around the boundary between FDTD and CIP regions

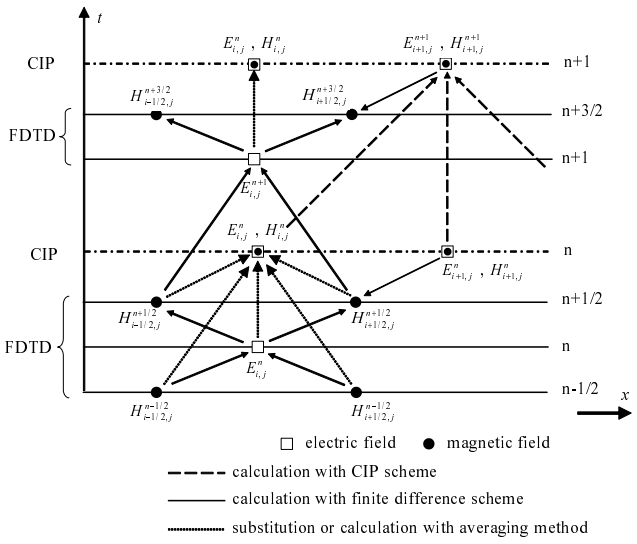

Fig. 3 diagram showing the calculation scheme of the fields around the boundary during the time development

4.1 Validation of proposed boundary condition

Numerical simulations of the present CIP-FDTD method are performed in a truncated analysis region of two-dimensional plane. The size of the plane is 800 × 400 cells. One half of the analysis region is the FDTD region, and the other is the CIP region. FDTD and CIP regions are seperated by the proposed boundary at the center as illustrated in Fig. 5. Two points s_1, s_2 are obsevation points of waveform at the location $x = 390\Delta x$, and $410\Delta x$. The reflection coefficient was calculated to confirm the validity of proposed method. In order to evaluate the reflected field from the boundary, an incident Gaussian plane wave was applied at $x = 350\Delta x$ in FDTD region. The first-order Mur's absorbing boundary condition was utilized to terminate the trancated

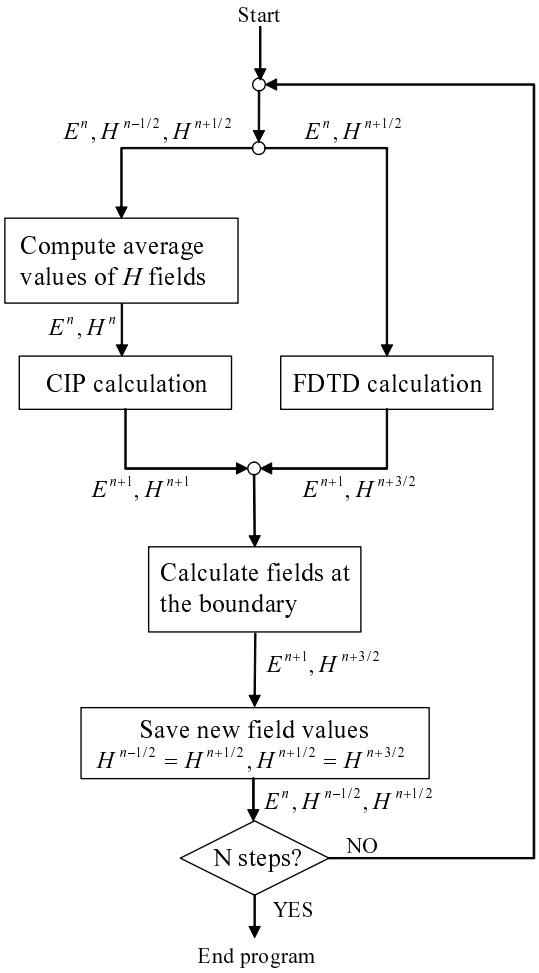

Fig. 4 Flowchart of the hybrid CIP-FDTD method

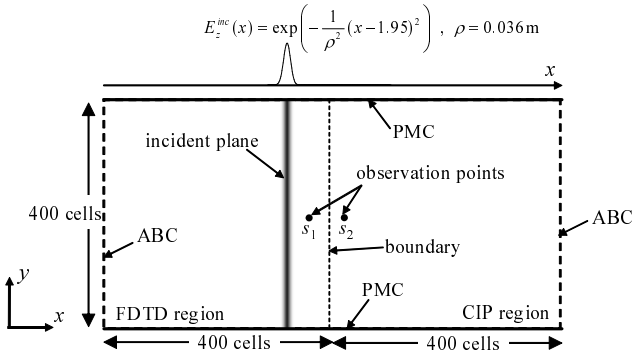

Fig. 5 Analysis model for the calculation of reflection from the boundary

space at the left and right boundary illustrated in the Fig 5. Although the problem is one-dimensional, two-dimensional numerical analysis was performed and the top and bottom boundaries are assumed to be perfect magnetic wall. In order to evaluate the field reflected by the boundary and transmitted into CIP region through the boundary, transmission and reflection coefficient defined by

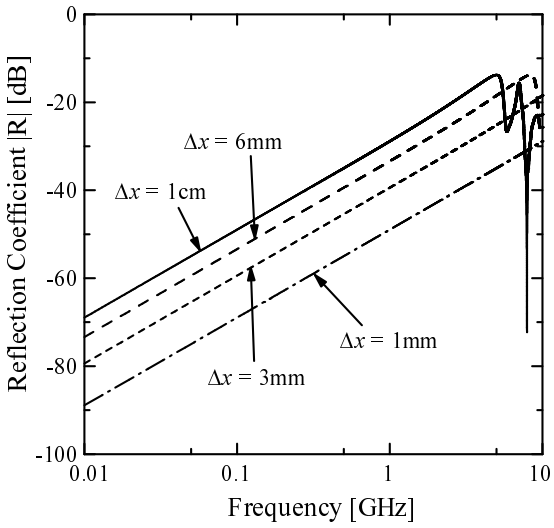

Fig. 6 Reflection coefficients of the CIP/FDTD boundary

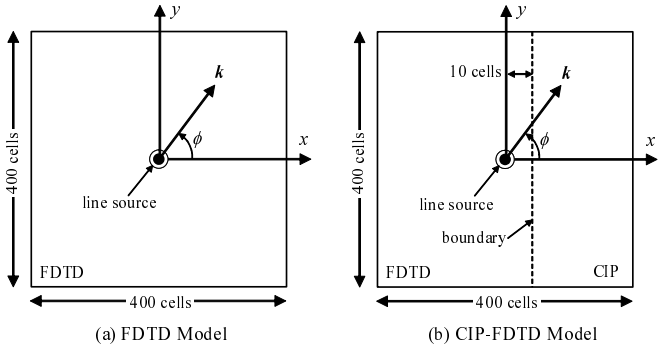

Fig. 7 Analysis model (a) FDTD Model (b) CIP-FDTD Model

$$T = \frac{\mathcal{F}(E_z^{CIP})}{\mathcal{F}(E_z^{inc})} \tag{16}$$

$$R = 1 - T = \frac{\mathcal{F}(E_z^{inc} - E_z^{CIP})}{\mathcal{F}(E_z^{inc})} \tag{17}$$

are used, where $\mathcal{F}(\cdot)$ denotes the Fourier transformation. E_z^{inc} and E_z^{CIP} were fields observed at the points s_1 and s_2 respectively. The reflection and transmission coefficients were normalized by the incident field.

The numerical results of the refection are shown in Fig. 6. The reflection coefficient increases as the frequency increases over broad ranges. The result shows that the electromagnetic waves can propagate from FDTD region into CIP region through the proposed boundary with the reflection coefficient smaller than -30dB below 10GHz when the cell size Δx is 1mm. The reflection coefficient increases as the cell size increases and is almost proportional to the cell size.

4. 2 Numerical dispersion error

In order to investigate the numerical dispersion error of each computation method, two-dimensional numerical analyses were performed. Fig.7 shows the model for analysis. The incident field was applied at the center of analysis space. The size of the analysis space is 400×400 cells with the same cell sizes $\Delta x = \Delta y = 6$mm. There is no need to trancate the analysis space with any boundary condition in the case of

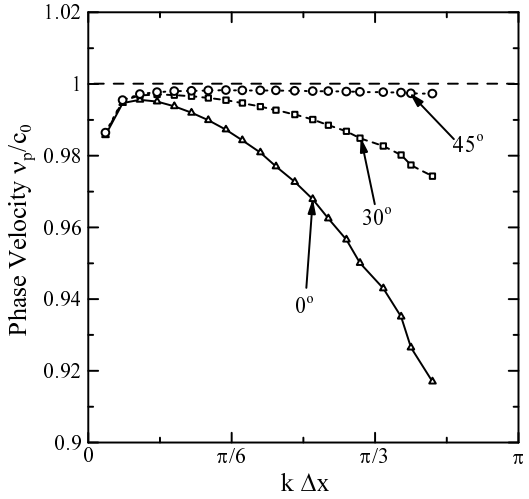

Fig. 8 Numerical phase velocity versus cell size of the FDTD method

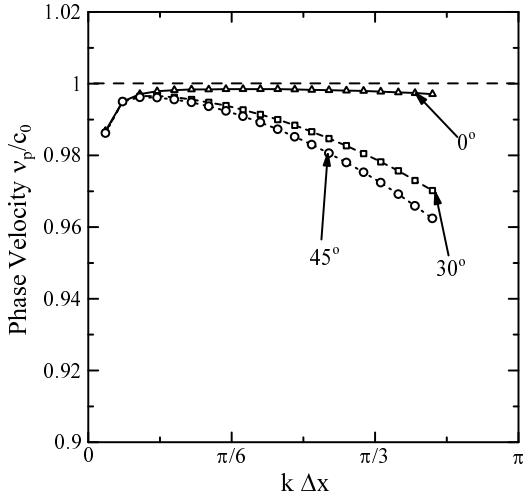

Fig. 9 Numerical phase velocity versus cell size of the CIP method

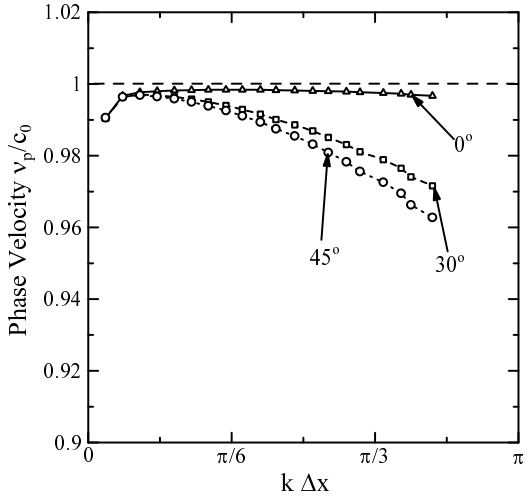

Fig. 10 Numerical phase velocity versus cell size of the CIP-FDTD method

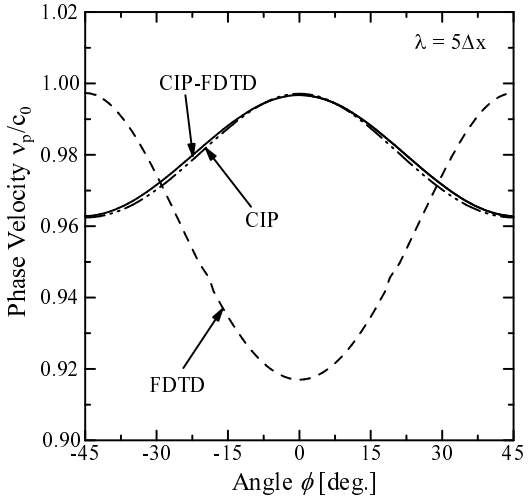

Fig. 11 Numerical phase velocity versus propagation angle at $\lambda = 5\Delta x$

CIP method. The discrete Fourier transform was performed at every point of calculation for the frequency from 0.5GHz to 10GHz with 0.5GHz interval.

Numerical phase velocity at different propagation angles of 0°, 30° and 45° direction in a two-dimensional analysis space is shown in Fig.8-10. respectively, whereas the worst velocity error occurs at 45° direction in FDTD method, the error is least in the 0° direction. The results for the cases of $\Delta = \Delta x = \Delta y = \lambda_0/20, \lambda_0/10$ and $\lambda_0/5$ are summarized in the Table 1. The velocity error of FDTD method for $\Delta = \lambda_0/5$ is 8.3%, at the direction of 45° which means that a sinusoidal numerical wave traveling over a $10\lambda_0$ distance would yield a lagging phase error of about 149.45°. These accumulative errors may be troublesome for the analysis of scattering structures involving phase cancellation such as the propagation characteristic analysis of MIMO (multiple-input multiple output) system. On the other hand, the CIP method has superior characteristics of dispersion error as illustrated in Fig. 9. The lagging phase for $10\lambda_0$ distance of propagation is only 66.9° in the worst case which is much less than that of the FDTD method.

Table. 1 The comparison of numerical phase errors between each method

		phase errors per one wavelength [deg.]		
		FDTD	CIP	CIP-FDTD
$\lambda = 25\Delta x$	0^o	0.88	0.38	0.36
	30^o	0.53	0.62	0.56
	45^o	0.40	0.69	0.62
$\lambda = 10\Delta x$	0^o	3.44	0.27	0.29
	30^o	1.12	1.54	1.51
	45^o	0.32	1.94	1.90
$\lambda = 5\Delta x$	0^o	14.94	0.52	0.59
	30^o	4.62	5.36	5.12
	45^o	0.48	6.76	6.69

The dispersion errors of the proposed CIP-FDTD method

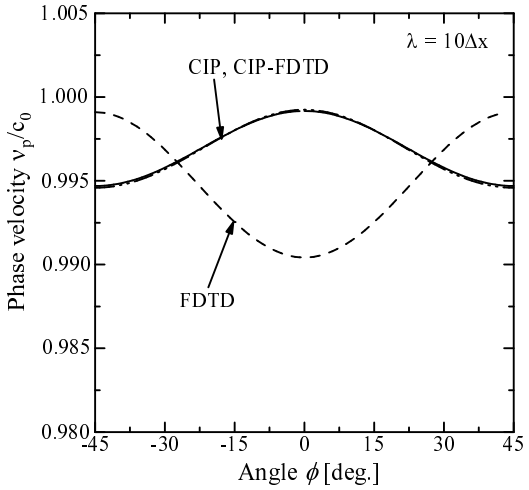

Fig. 12 Numerical phase velocity versus propagation angle at $\lambda = 10\Delta x$

is shown in Fig.10. CIP-FDTD method yields the similar phase error with CIP method. The numerical phase velocity versus propagation angle in the cases $\lambda = 10\Delta x$ and $\lambda = 5\Delta x$ are shown in Fig.12 and Fig.11, respectively. When $\lambda = 10\Delta x$, the worst error in FDTD occurs at $\theta = 0^o$, which is about 1% delay from the normal light velocity in the vacuum. However, the worst errors of CIP and CIP-FDTD occurs at $\theta = 45^o$, with the phase velocity error about 0.5% which is about half of FDTD result. Thus, it is proved that the CIP-FDTD yields better propagation characteristics than that of FDTD.

5. Concluding remarks

In this paper, a hybrid CIP-FDTD method is proposed as a new technique to solve a problem of the large or long distance propagation with an antenna included in the analysis space. The boundary conditions between the FDTD method and the CIP method was considered and implemented to maintain the continuity of the fields by utilizing the averaging value of magnetic fields. When an incident field is applied in the FDTD region, the numerical reflection coefficient of the electric fields is significantly small in the case an incident field is applied in the FDTD region. Furthermore, the phase error of the FDTD, CIP, and hybrid method was investigated. The results verify that the CIP-FDTD method yields small phase error similar to CIP method. The proposed method can be extended to the three-dimensional problem which will be further investigated in the future.

References

[1] K.S.Yee, "Numerical Solution of Initial Boundary Value Problems Involving Maxwell 's Equations in Isotropic Media," IEEE Trans. Antennas Propagat., vol.14, no.4, pp.302-307, 1996

[2] A. Taflove, "Computational Electrodynamics, The Finite-Difference Time-Domain Method" Artech House Publisher, 1995

[3] M.F.Fadi and M.Piket-May, "A Modified FDTD(2,4) scheme for modeling electrically large structures with high-phase accuracy," IEEE Trans. Antennas Propagat., vol.45, no.2, pp.254-264, 1997

[4] K.Lan, Y.Liu, and W.Lin, "A Higher Order (2,4) Scheme for Reducing Dispersion in FDTD Algorithm," IEEE Trans. Electromagn. Compat., vol.41, no.2, pp.160-165, may 1999

[5] C.W.Manry Jr, S.L.Broschat, and J.B.Schneider, "Higher-Order FDTD Methods for Large Problems," J.Appl. Comput. Electromag. Soc., vol.10, no.2, pp.17-29, 1995

[6] Y.Ogata, T.Yabe, K.Odagaki, "An Accurate Numerical Scheme for Maxwell Equation with CIP-Method of Characteristics," Commun. Comput. Phys., vol.1, no.2, pp.311-335, april 2006

[7] T.Nakamura, R.Tanaka, T.Yabe, K.Takizawa, "Exactly Conservative Semi-Lagrangian Scheme for Multi-dimensional Hyperbolic Equations with Directional Splitting Technique," J. Comput. Phys., vol.174, pp.171-207, 2001

[8] F.Xiao, T.Yabe, "Completely Conservative and Oscillationless Semi-Lagrangian Schemes for Advection Transportation," J. Comput. Phys., vol.170, pp.498-522, 2001

[9] T.Utsumi, T.Kunugi, T.Aoki, T.Yabe, "Stability and accuracy of the Cubic Interpolated Propagation scheme," Comput. Phys. Commun., vol.101, pp.9-20, 1997

[10] T.Yabe, K.Takizawa, M.Chino, M.Imai, and C.C.Chu, "Challenge of CIP as a universal solver for solid liquid and gas," Int. J. Numer. Methods Fluids, vol.47, pp.655-676, 2005

[11] S.Watanabe, O.Hashimoto, "An Examination about Method for Analyzing Electromagnetic Field Using CIP Method," IEICE Tech. Report, EMCJ2005-37, pp.91-95, June 2005

[12] Y.Yoshida, K.Okubo, N.Takeuchi, "The Type-C CIP Electromagnetic Field Analysis," IEICE Tech. Report, AP2006-70, pp.7-12, September 2006

[13] K.Okubo, N.Takeuchi, "Numerical Analysis of Electromagnetic Field Generated by Line Current Using the CIP Method," IEICE Tech. Report, AP2004-336, pp.197-202, March 2005

[14] K.Okubo, N.Takeuchi, "A Consideration on Application of Time Domain Numerical Analysis Using CIP Method to Electromagnetic Fields," IEICE Tech. Report, AP2005-84, pp.7-12, October 2005

[15] Y.Ogata, T.Yabe, K.Odagaki, "An Accurate Numerical Scheme for Maxwell Equation with CIP-Method of Characteristics", Comm. Comput. Phys., Vol.1, No.2, pp.311-335, April 2006

[16] J.S.Shang, "A Fractional-Step Method for Solving 3D, Time-Domain Maxwell Equations," J. Comp. Phys., vol.118, pp.109-119, 1995

[17] P.K.Smolarkiewicz and J.A.Pudykiewicz, "A Class of Semi-Lagrangian Approximations for Fluids," J. Atmospheric Sci., vol.49, pp.2028-2096, 1992